FIGURE 1

Gas Holdup for Various Aqueous Systems

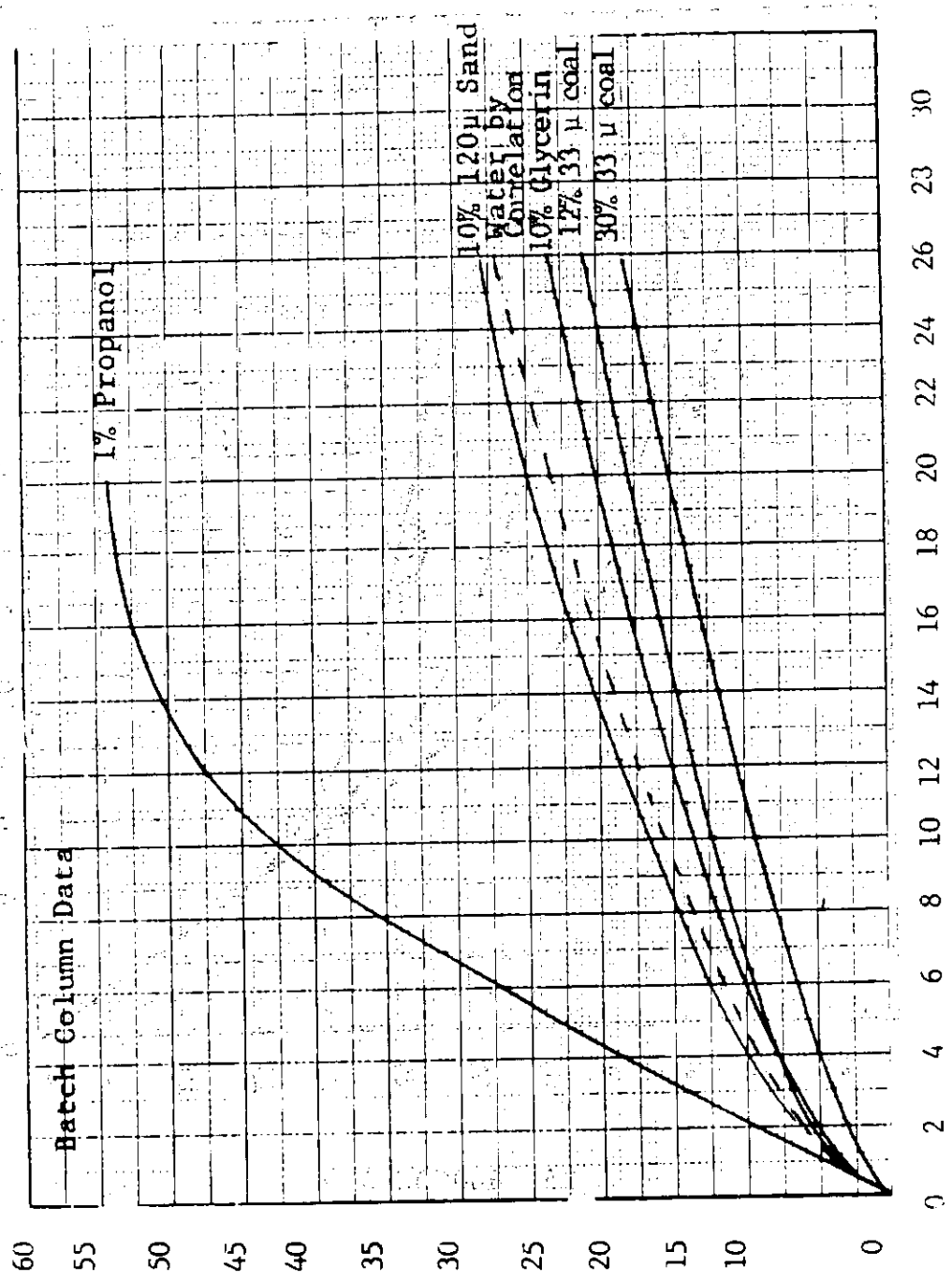

FIGURE 2

Gas Holdup for Dilute Alcohol Solutions

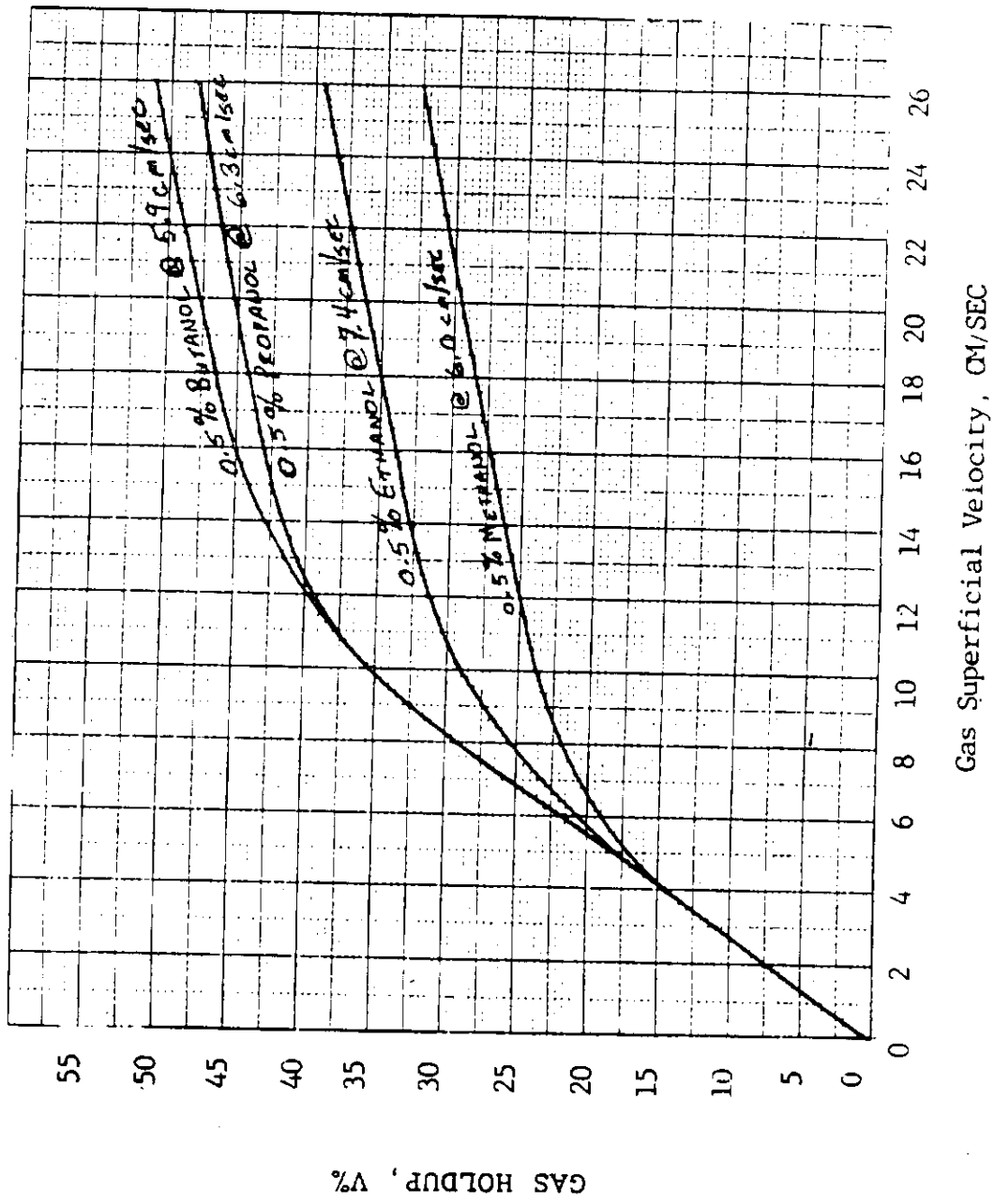

FIGURE 3

Effect of Surface Tension on Gas Holdup
for Dilute Alcohol Solutions

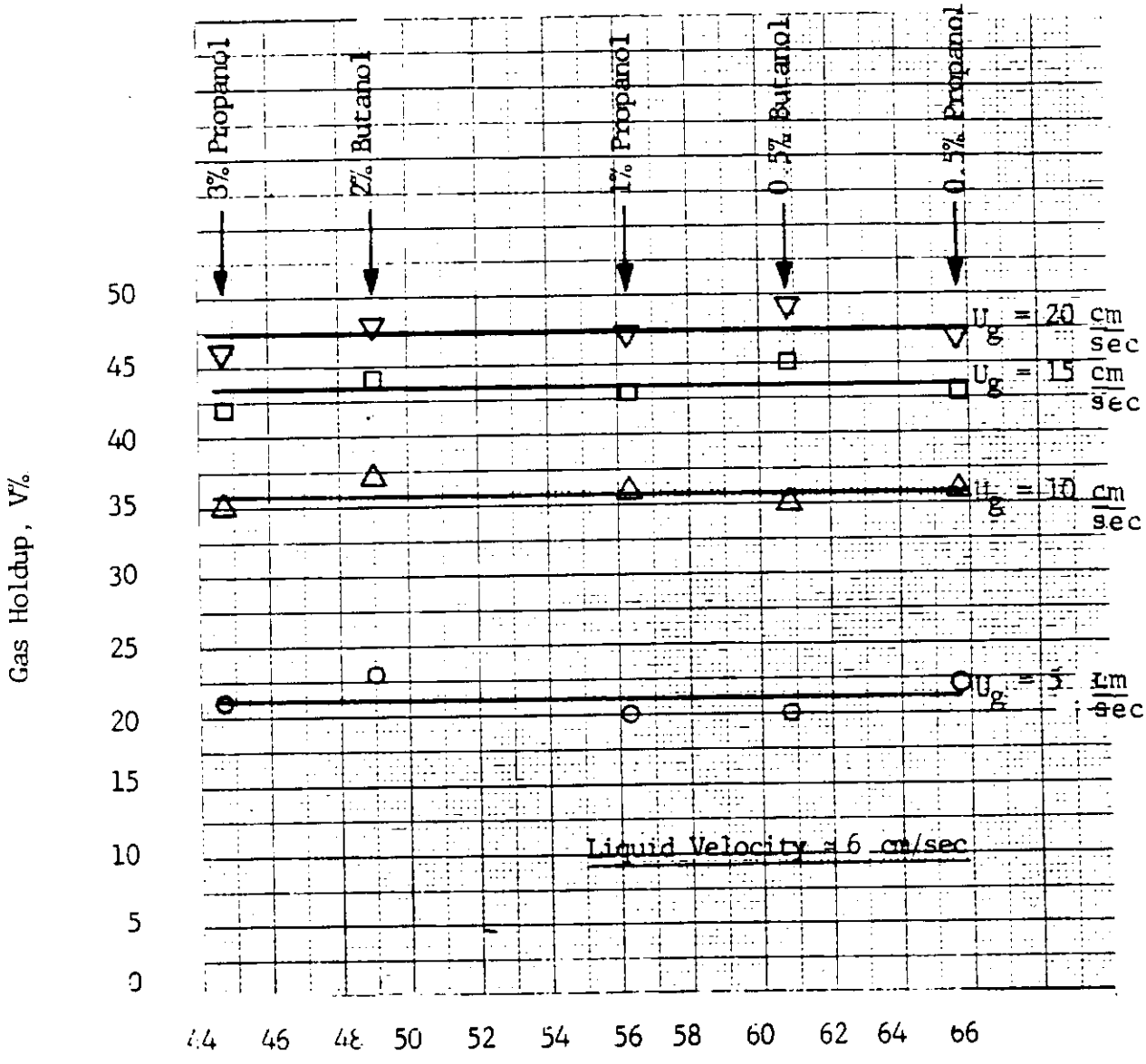

FIGURE 4

Effect of Liquid Phase Superficial Velocity on Gas Holdup

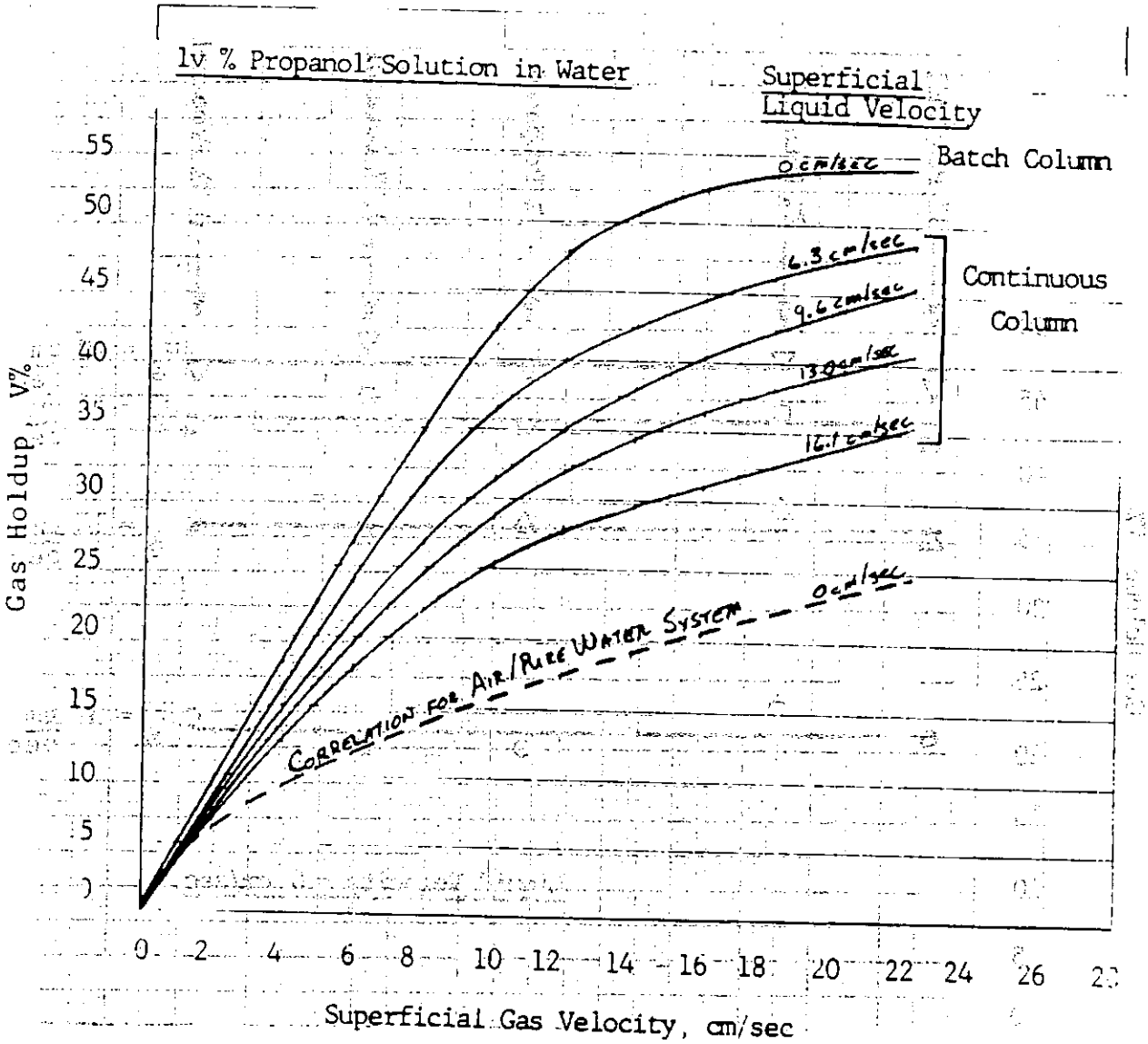

FIGURE 5

Concentration Curves For Axial Dispersion

Model In An "Open Vessel" System

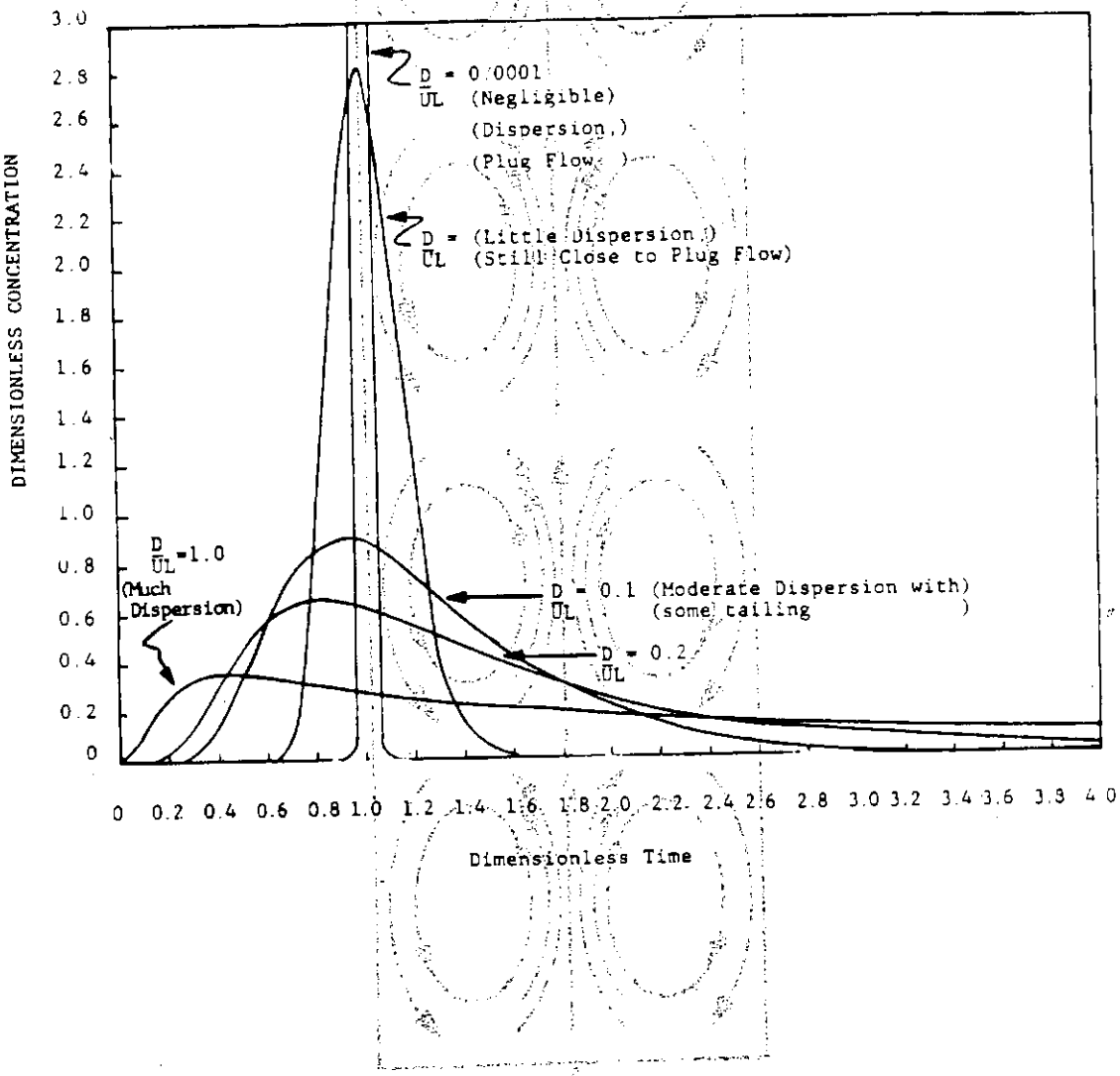

FIGURE 6

Representation of Churn Turbulent Flow with Internal Recirculation Cells - Cocurrent Upflow Bubble Column

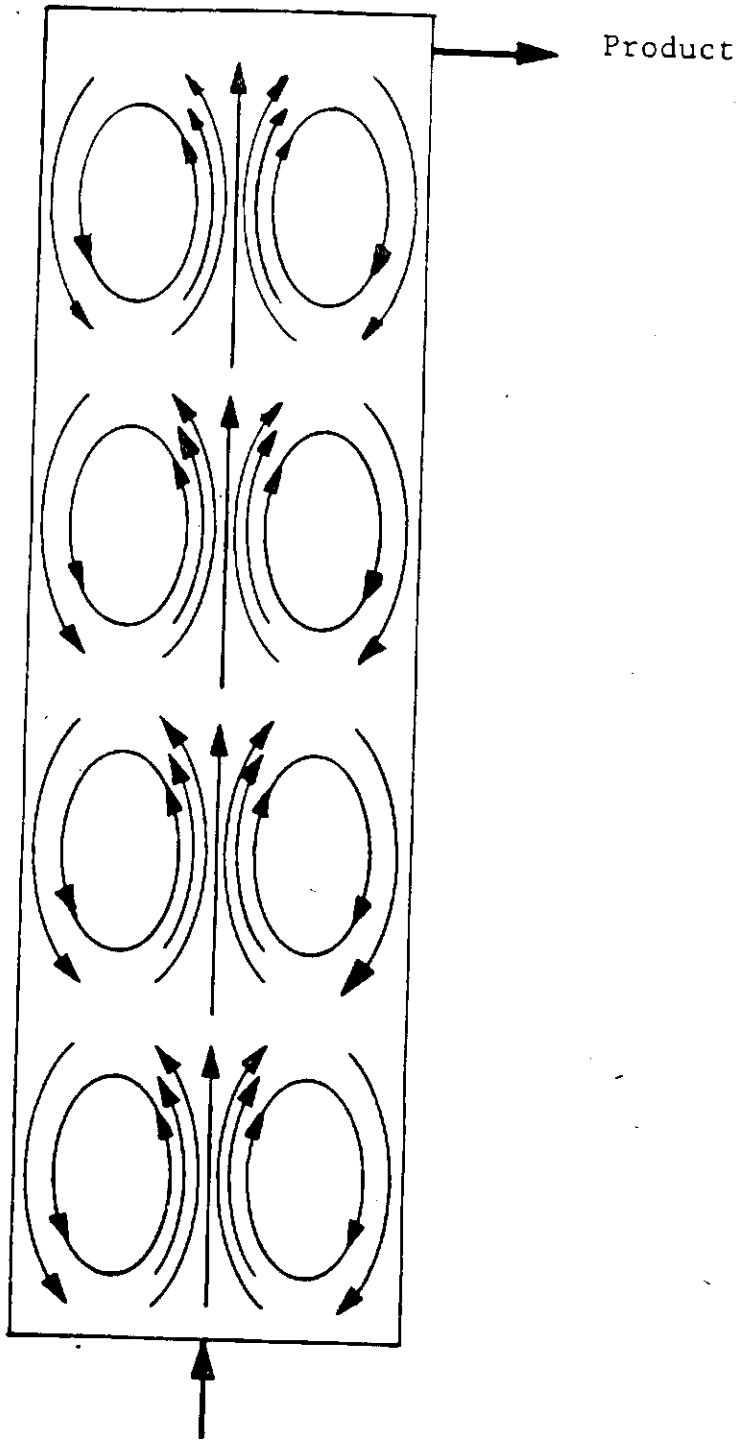

FIGURE 7

Possible Flow Models for an SRC-II Dissolver

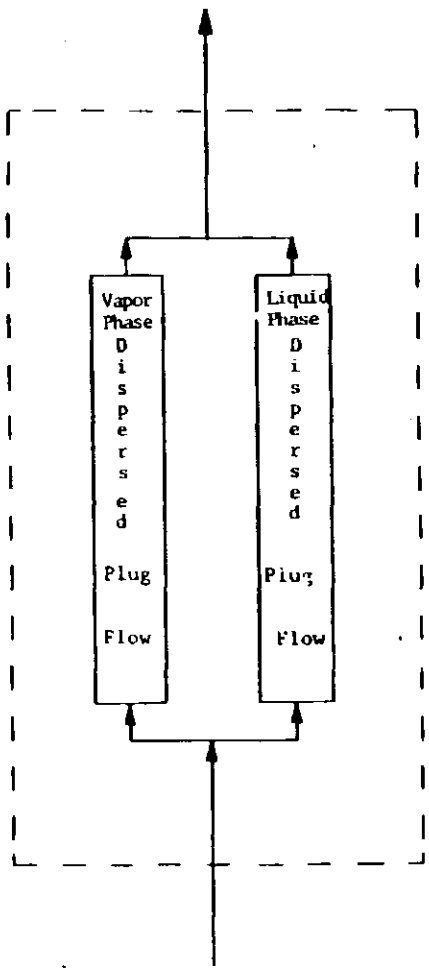

Axial Dispersion Model for both Phases

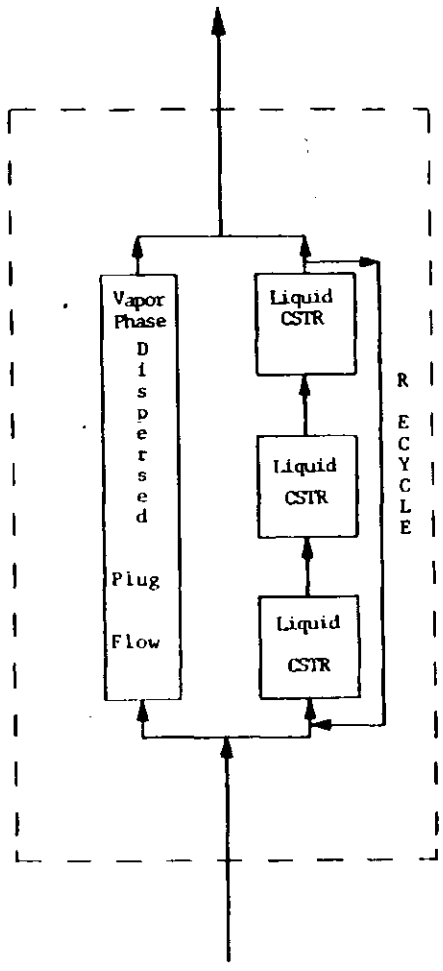

Tanks-in-Series Model for Liquid Axial Dispersion Phase Model for Vapor Phase

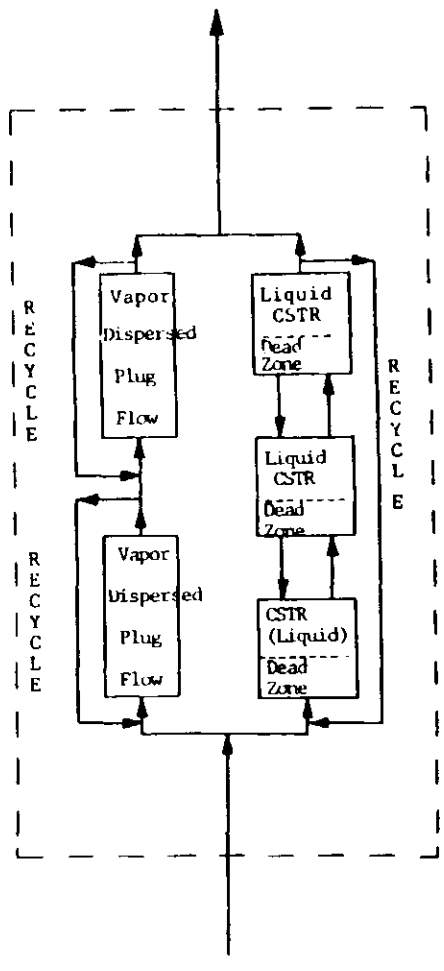

Multiparameter Model

FIGURE 8

Ft. Lewis Dissolver

Radiotracer Detector Locations

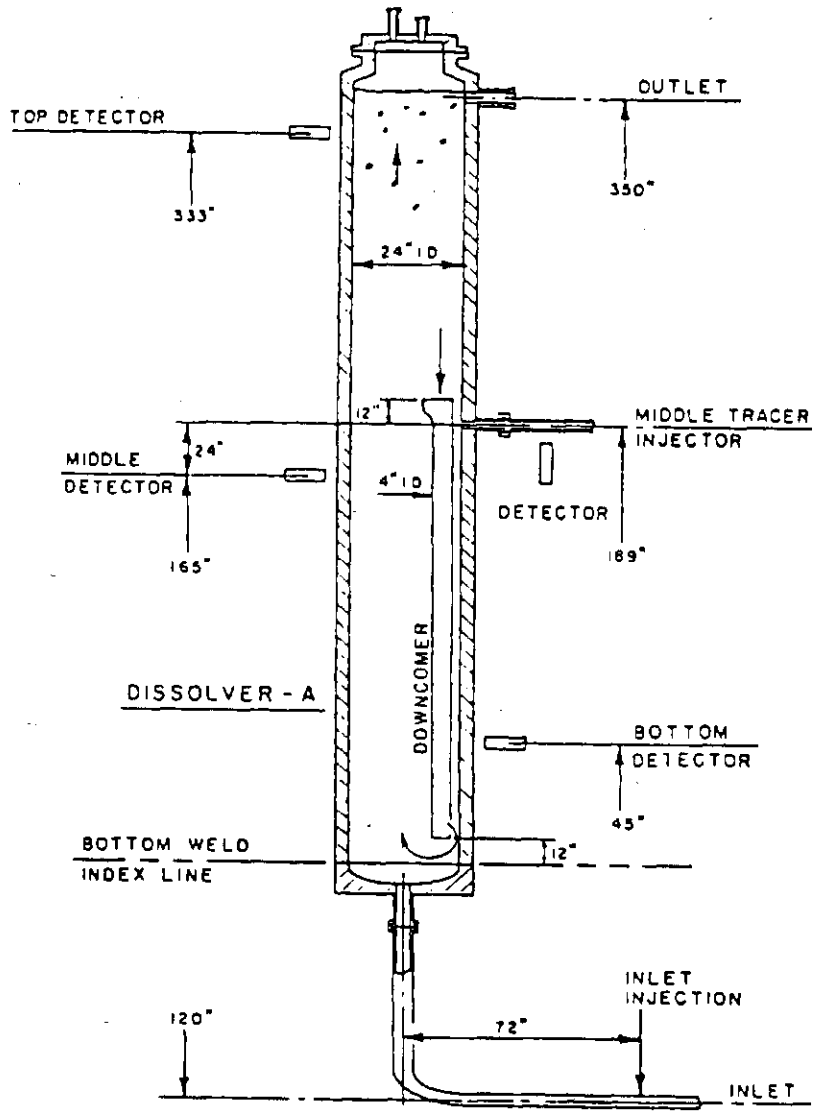

FIGURE 9

Top Detector response to a liquid phase radiotracer Injection at the Dissolver Inlet

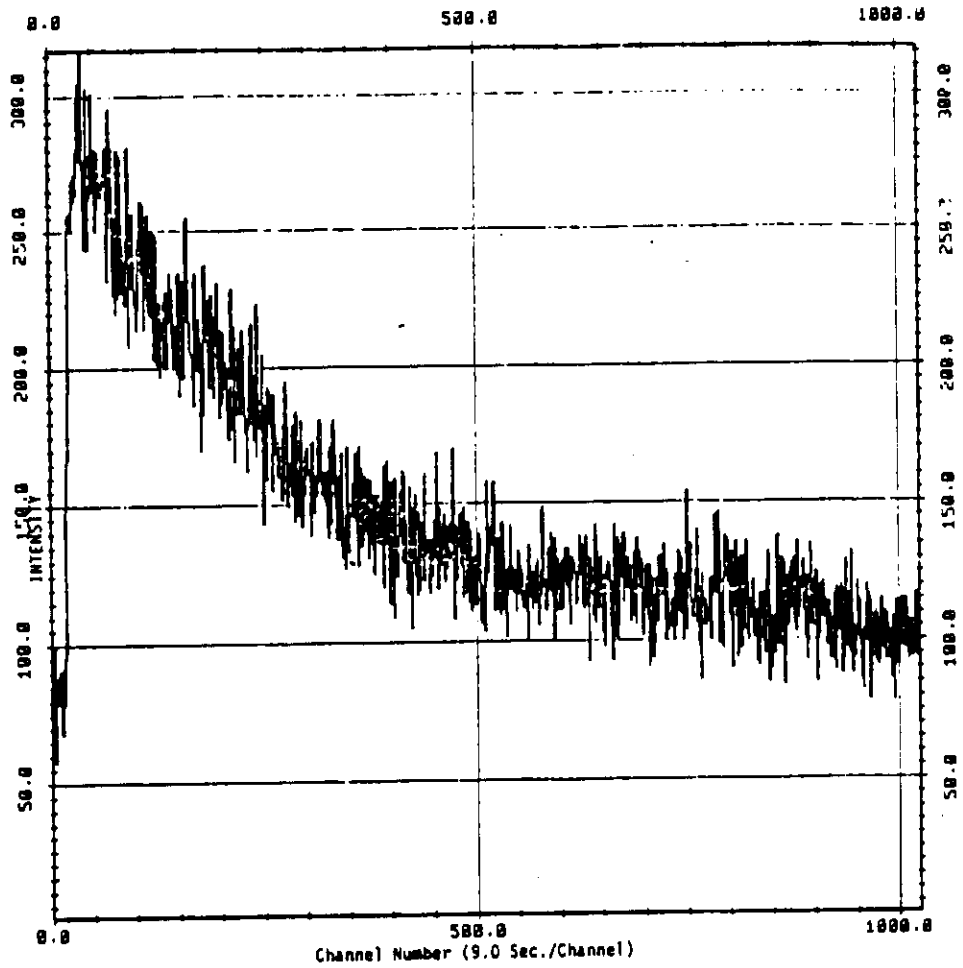

FIGURE 10

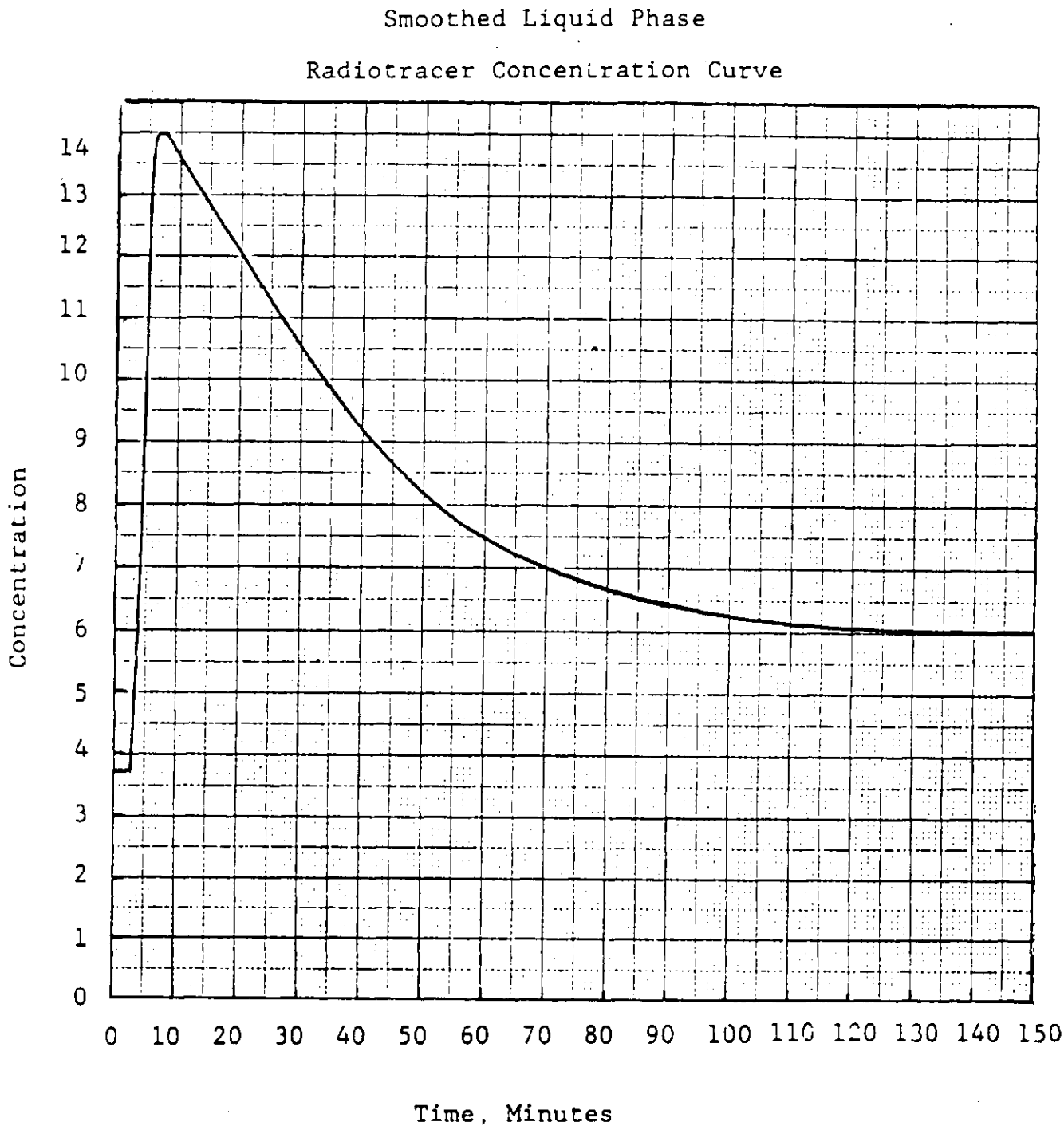
Smoothed Liquid Phase
Radiotracer Concentration Curve
Concentration
0
1
2
3
4
5
6
7
8
9
10
11
12
13
14
0 10 20 30 40 50 60 70 80 90 100 110 120 130 140 150
Time, Minutes

FIGURE 11

Alternate Baselines for Liquid Phase

Radiotracer Concentration Curve

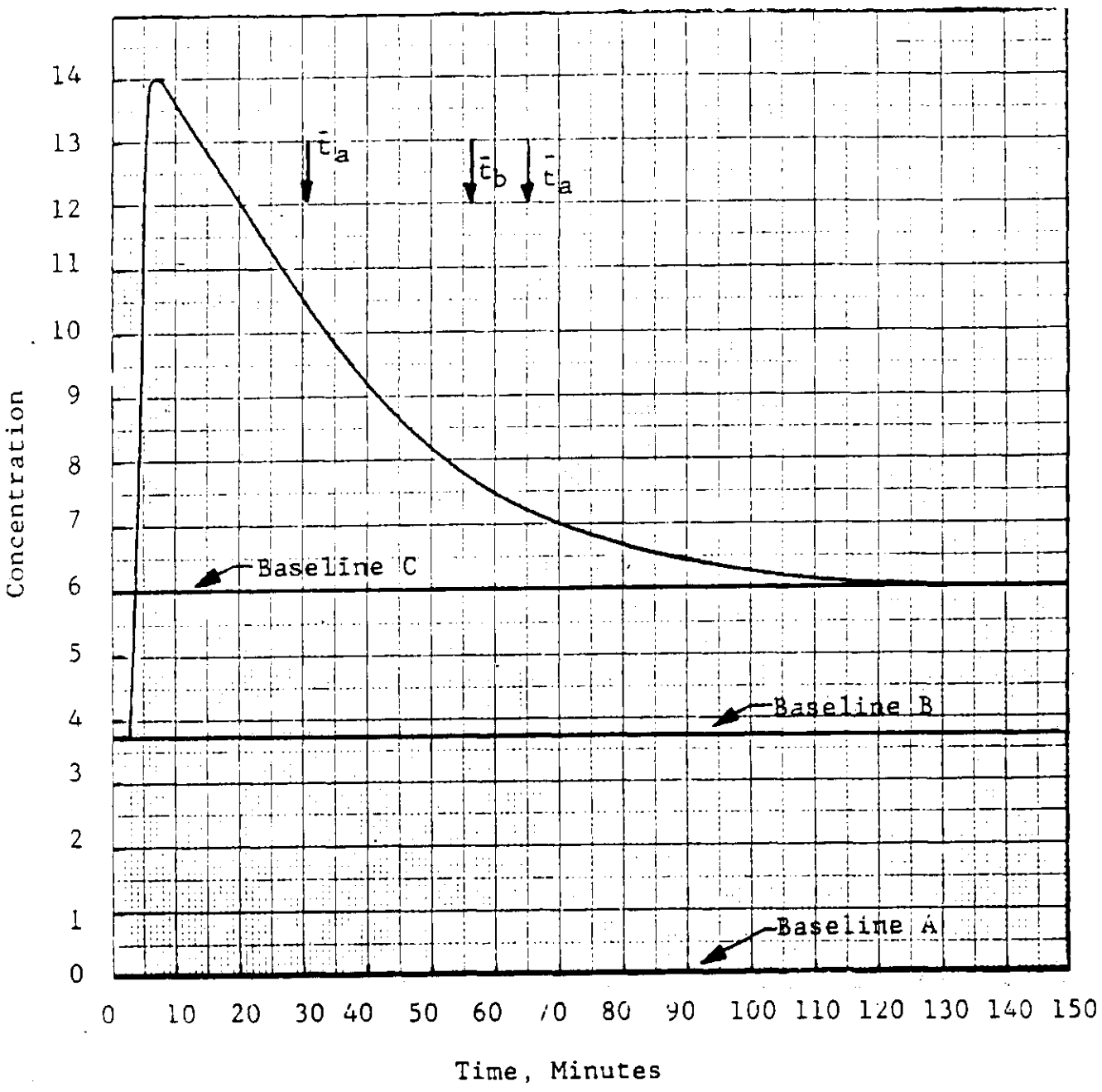

FIGURE 12

Predicted Concentration Curve for Baseline A

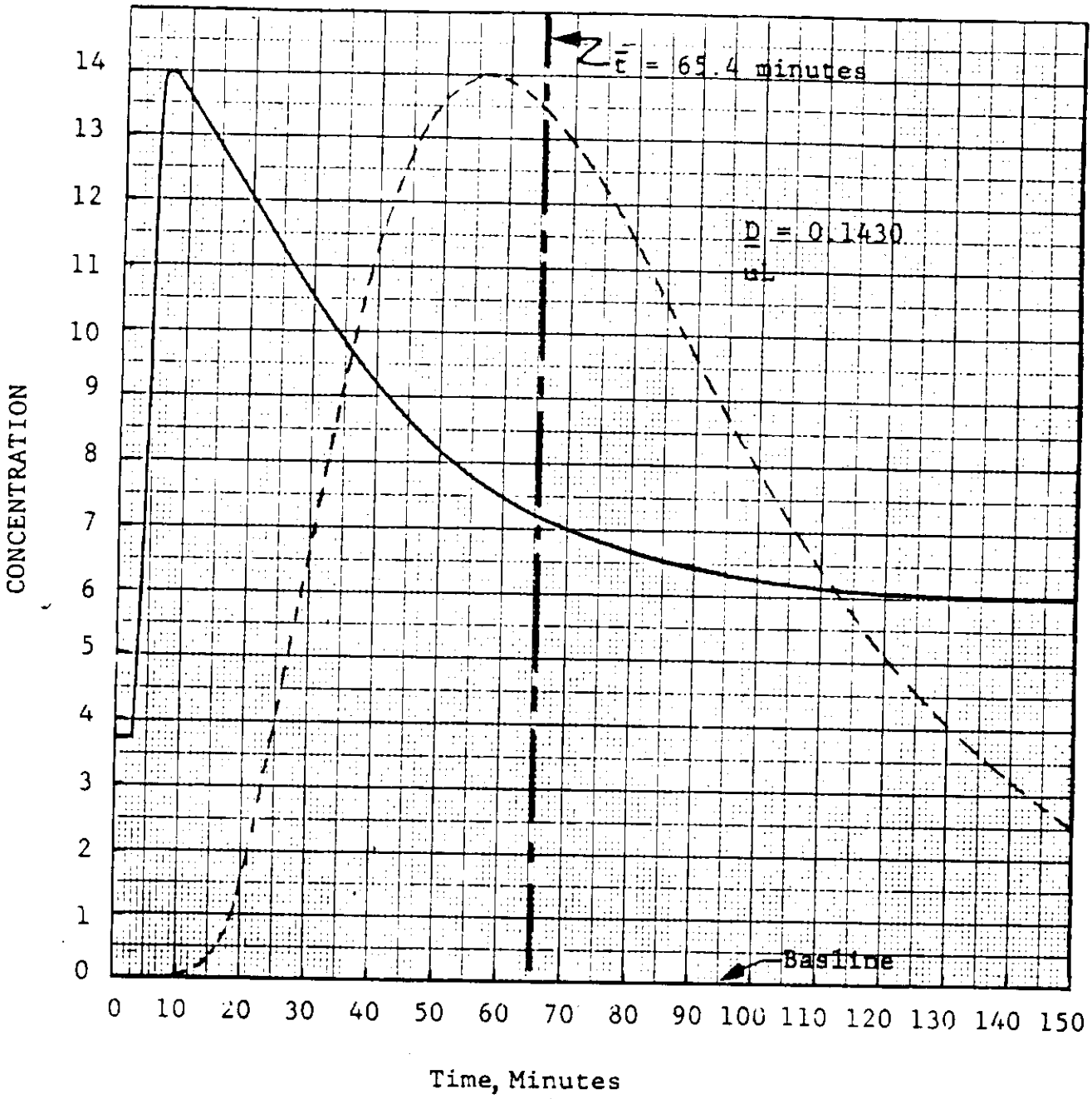

FIGURE 13

Predicted Concentration

Curve for Baseline B

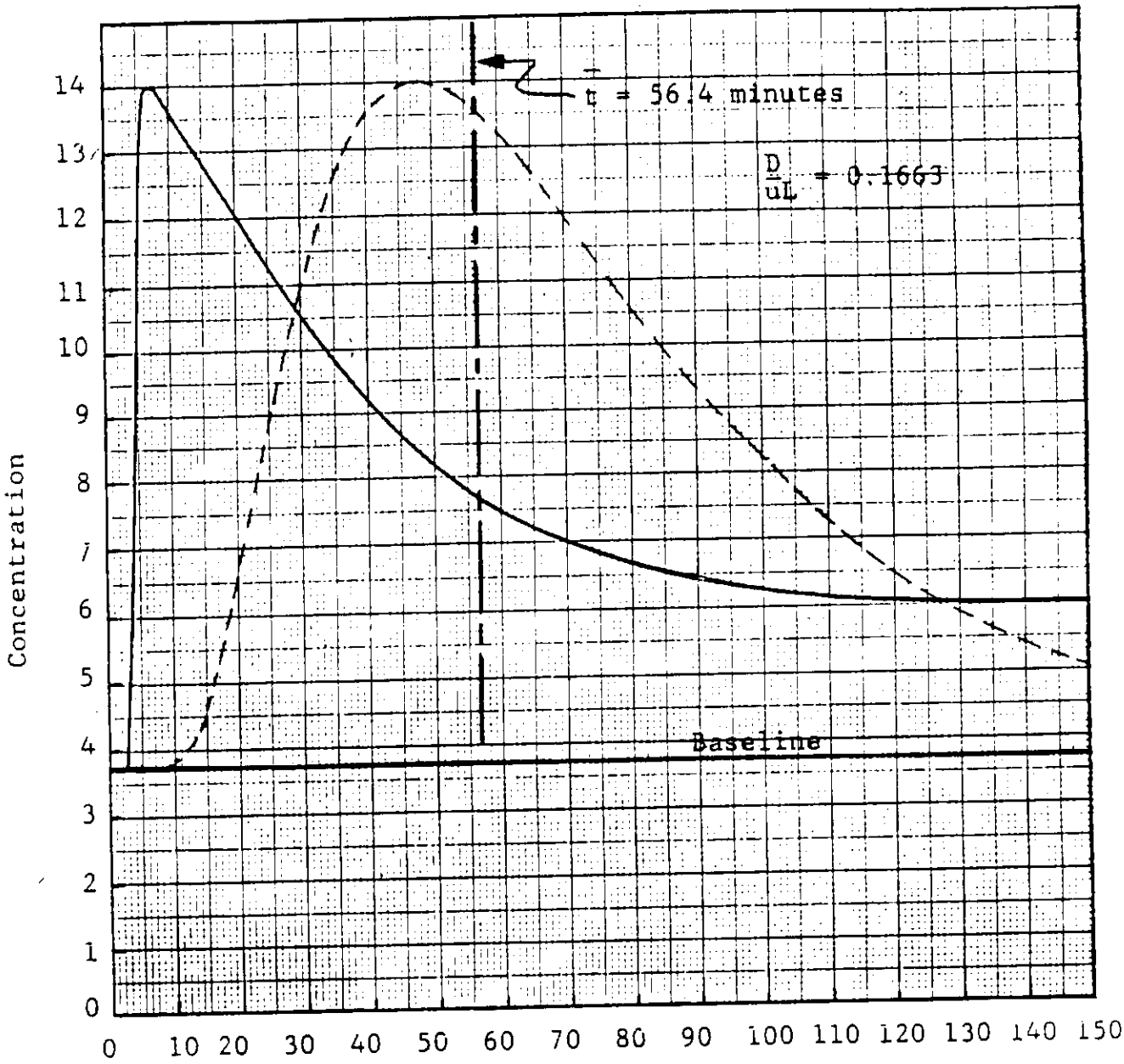

FIGURE 14

Predicted Concentration
Curve for Baseline C

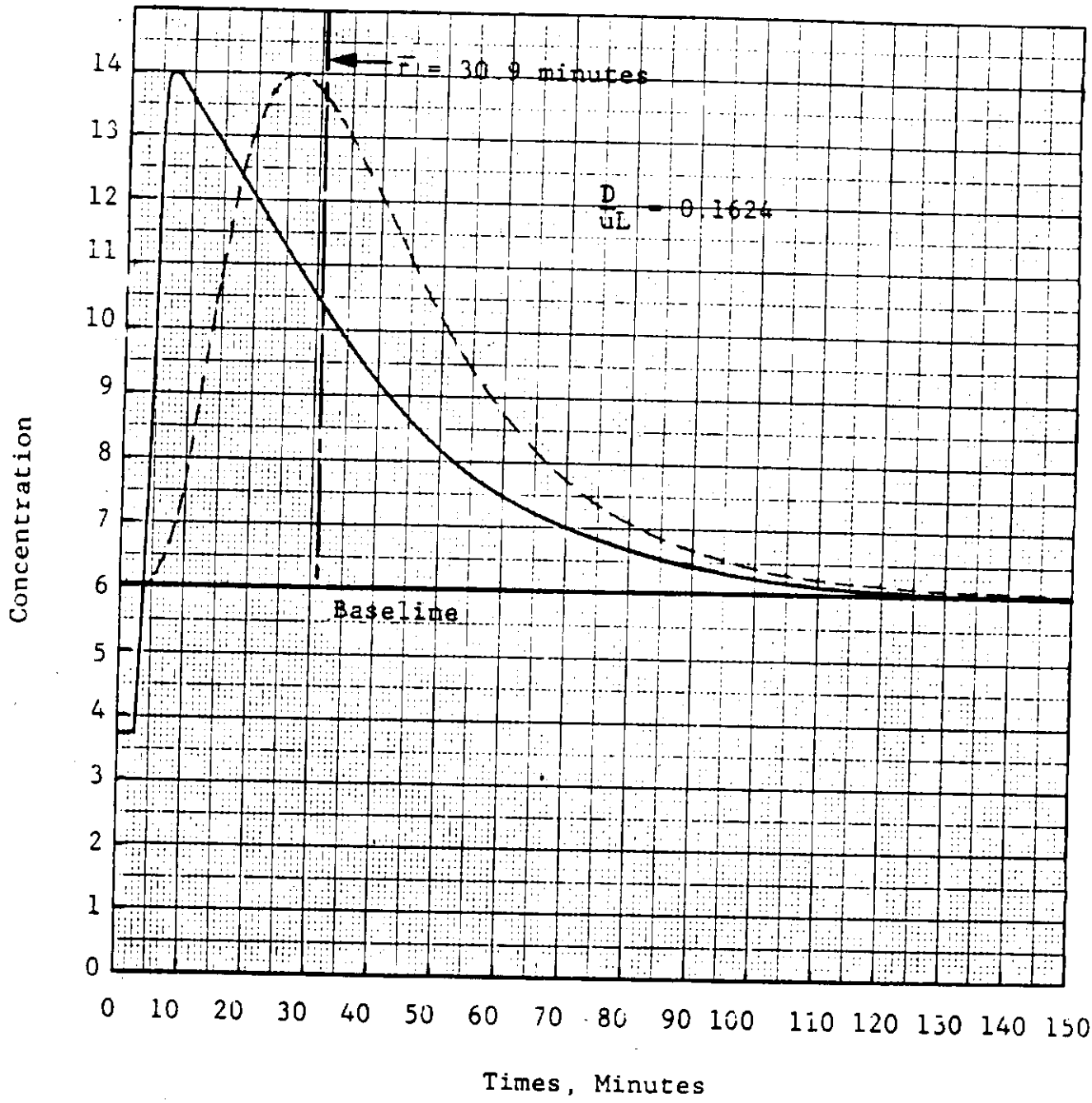

FIGURE 15

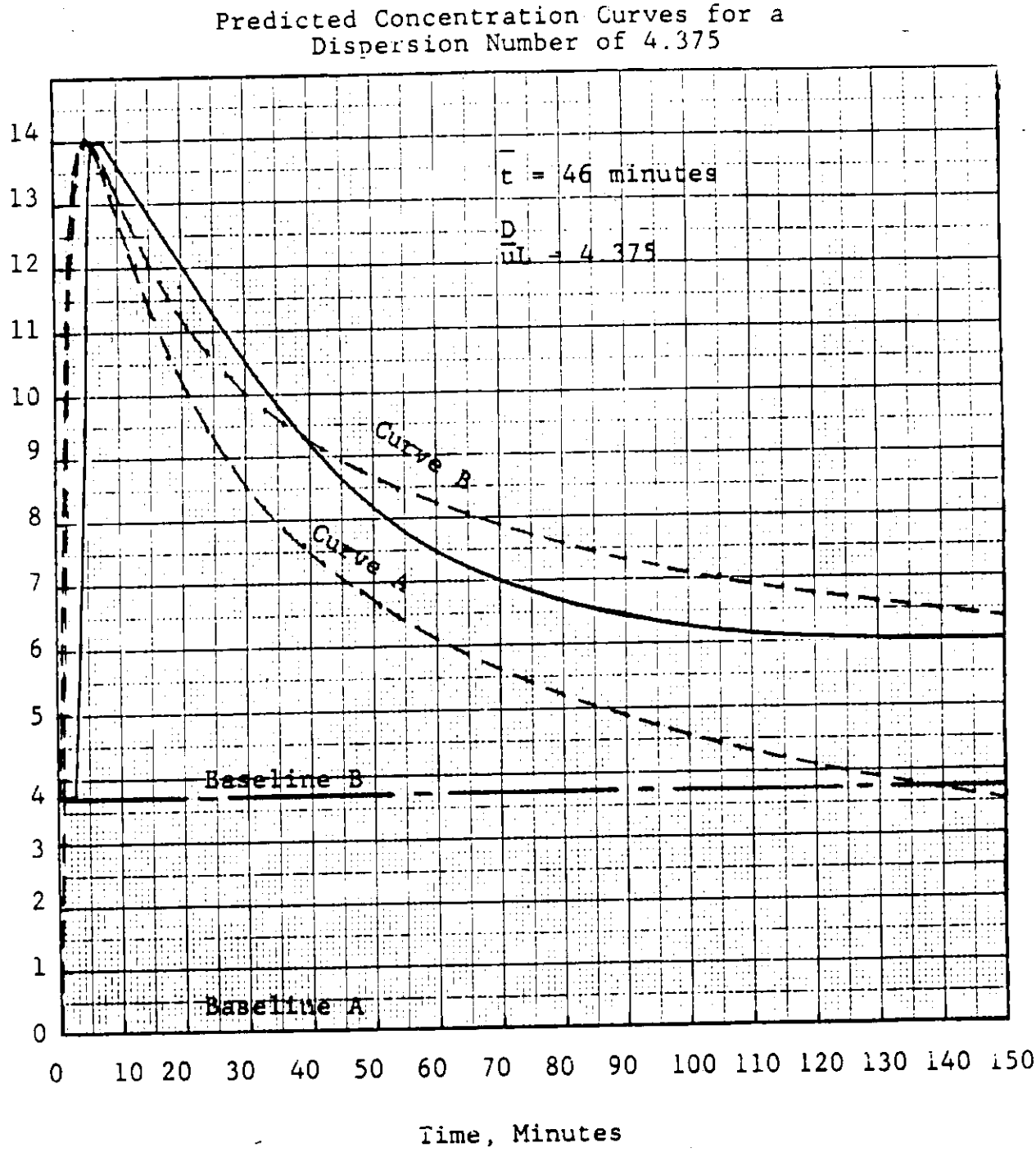
Predicted Concentration Curves for a
Dispersion Number of 4.375
$\bar{t}$ = 46 minutes
$\frac{D}{uL}$ = 4.375
Curve B
Curve A
Baseline B
Baseline A
0
1
2
3
4
5
6
7
8
9
10
11
12
13
14
0 10 20 30 40 50 60 70 80 90 100 110 120 130 140 150
Time, Minutes

FIGURE 16

Top Detector Response to a Gas Phase
Radiotracer Injection at the Dissolver Inlet

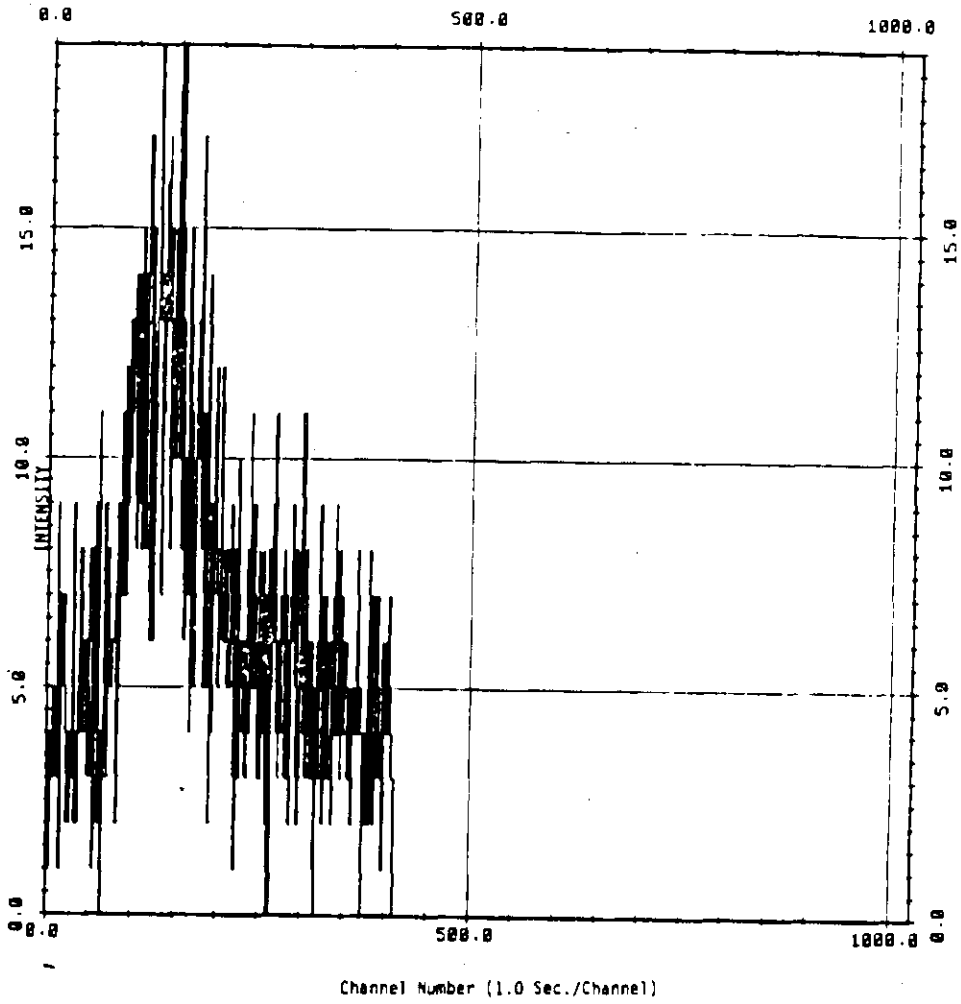

FIGURE 17

Flow Regime Transition
for Dilute Alcohols

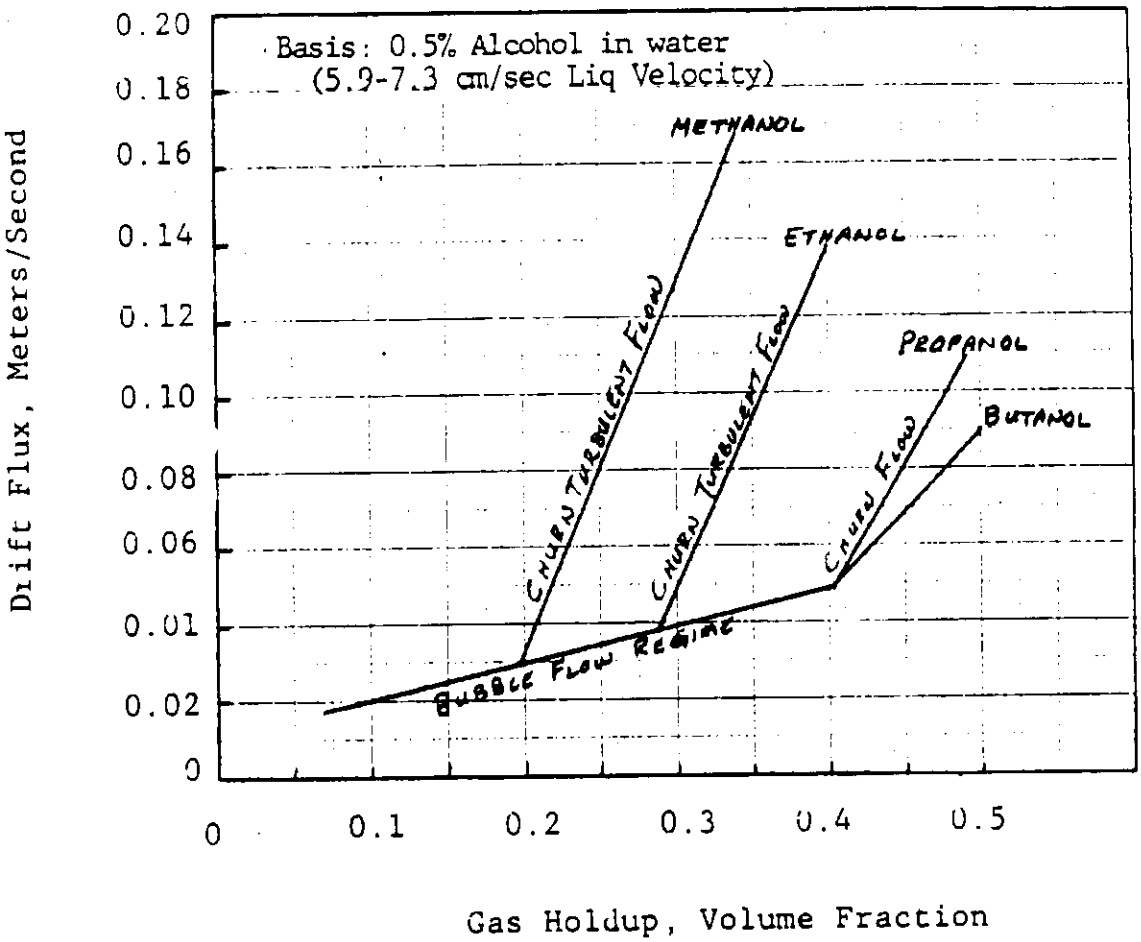

FIGURE 18

Flow Regime Transition for
Different Concentrations of Electrolyte

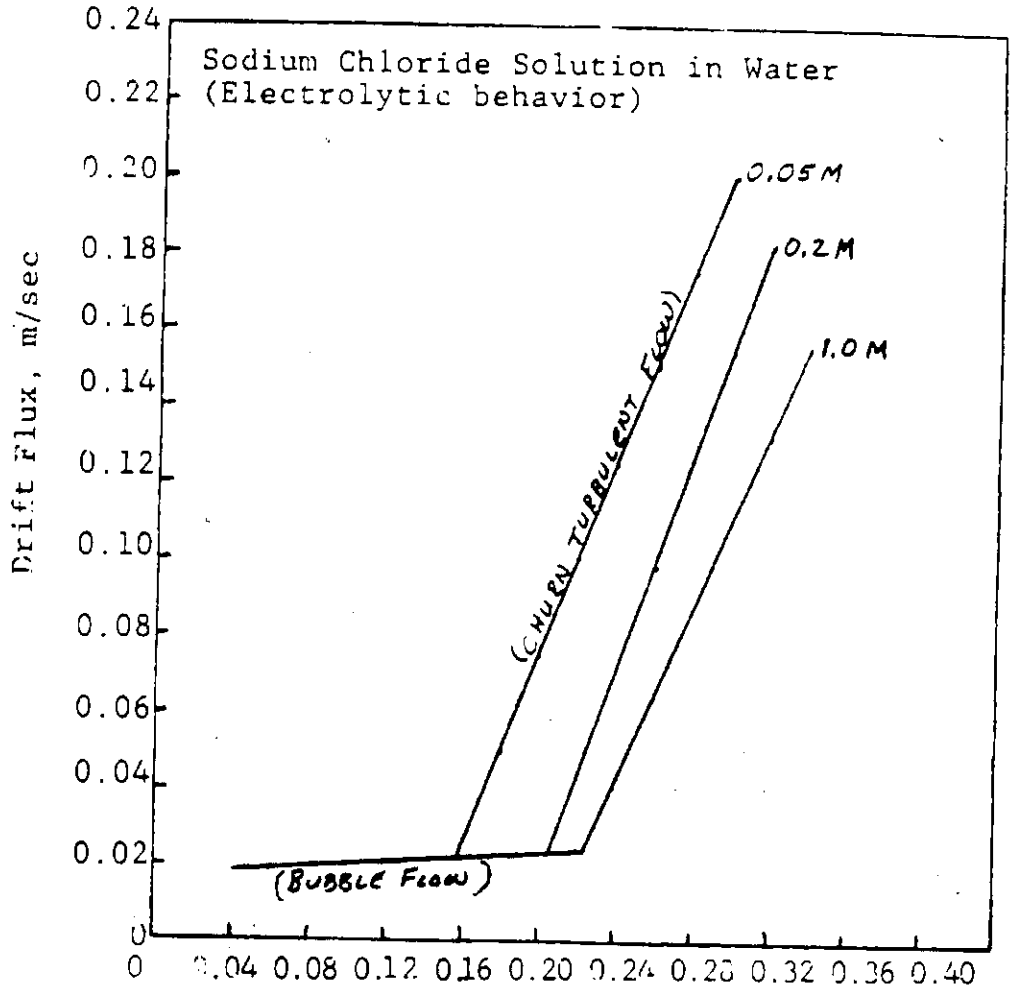

FIGURE 19

FLOW REGIME TRANSITION

FOR DIFFERENT DEGREES OF VISCOELASTICITY

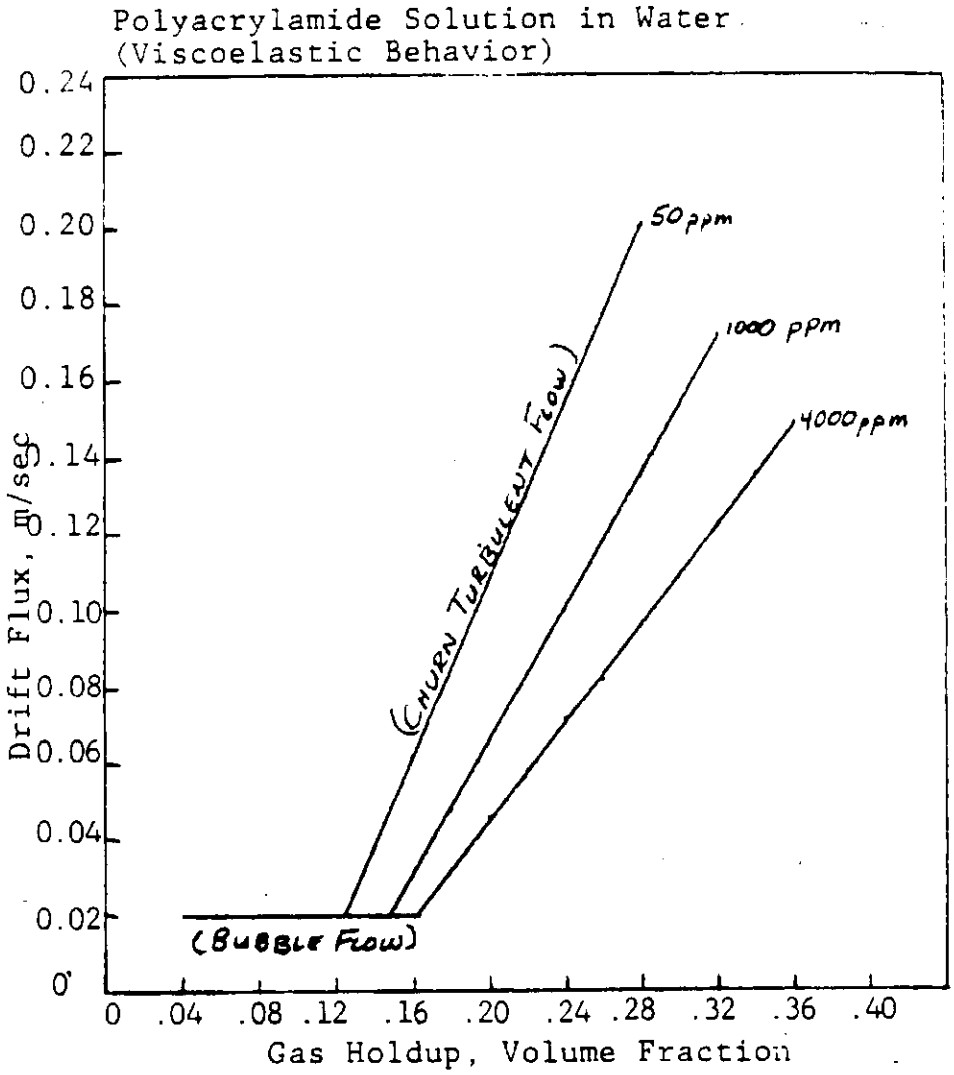

FIGURE 20

FLOW REGIME TRANSITION

FOR DIFFERENT DEGREES OF PSEUDOPLASTIC BEHAVIOR

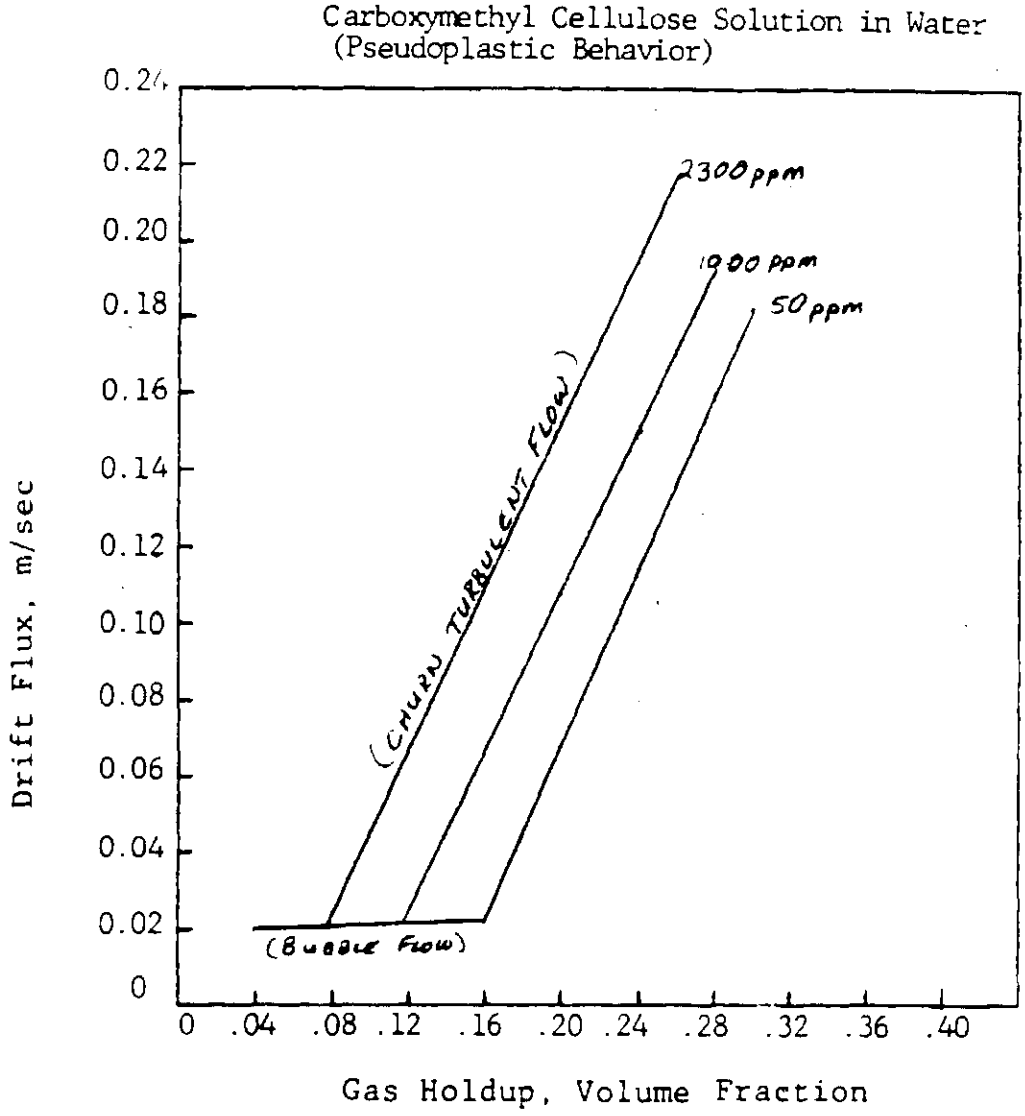

FIGURE 21

RELATIONSHIP BETWEEN DISPERSION COEFFICIENT

AND FLOW REGIME

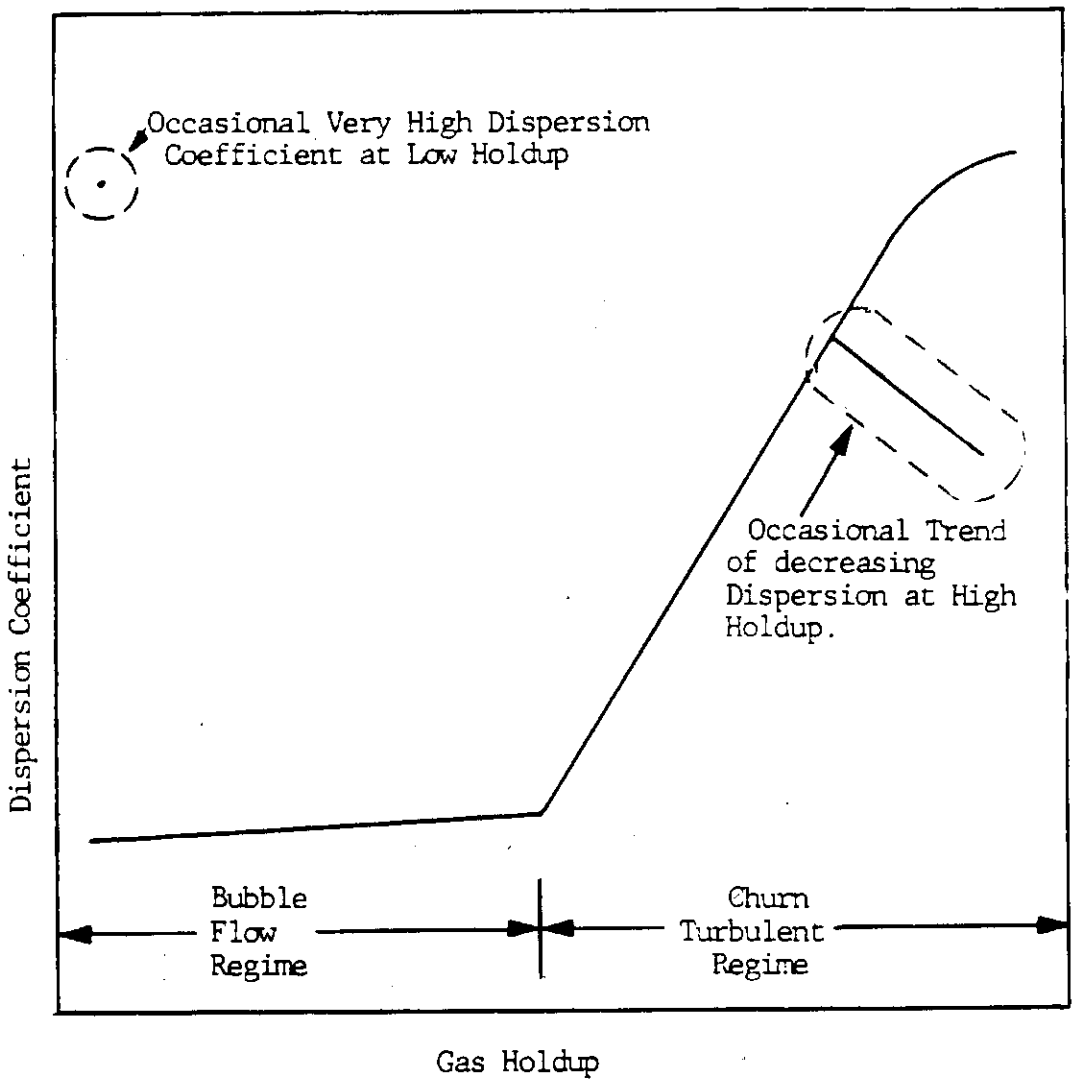

FIGURE 22

SIMPLIFIED SRC REACTION MODEL

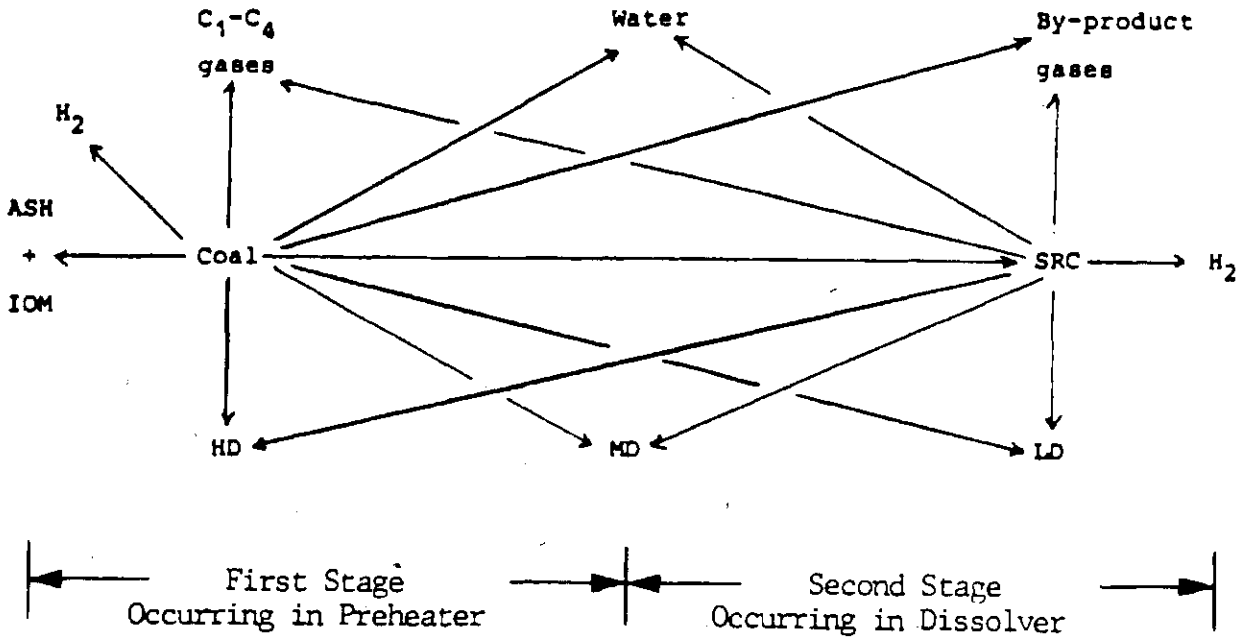

Second Stage Reaction Rate Equation:

$$r_{SRC} = 8.256 \times 10^4 \exp(-18900/RgT) \cdot P_{H_2}^{0.28} \cdot X_{ash}$$

where r_{SRC} is the rate of conversion of SRC, kg of SRC/(litre hr); P_{H_2} is the partial pressure of hydrogen, atms; X_{ash} is the mass fraction of ASH in the reactor; Rg is the universal gas constant; and T is the absolute temperature of reaction, °K.

FIGURE 23

HEAT OF REACTION

BASED ON P-99 HEAT BALANCES

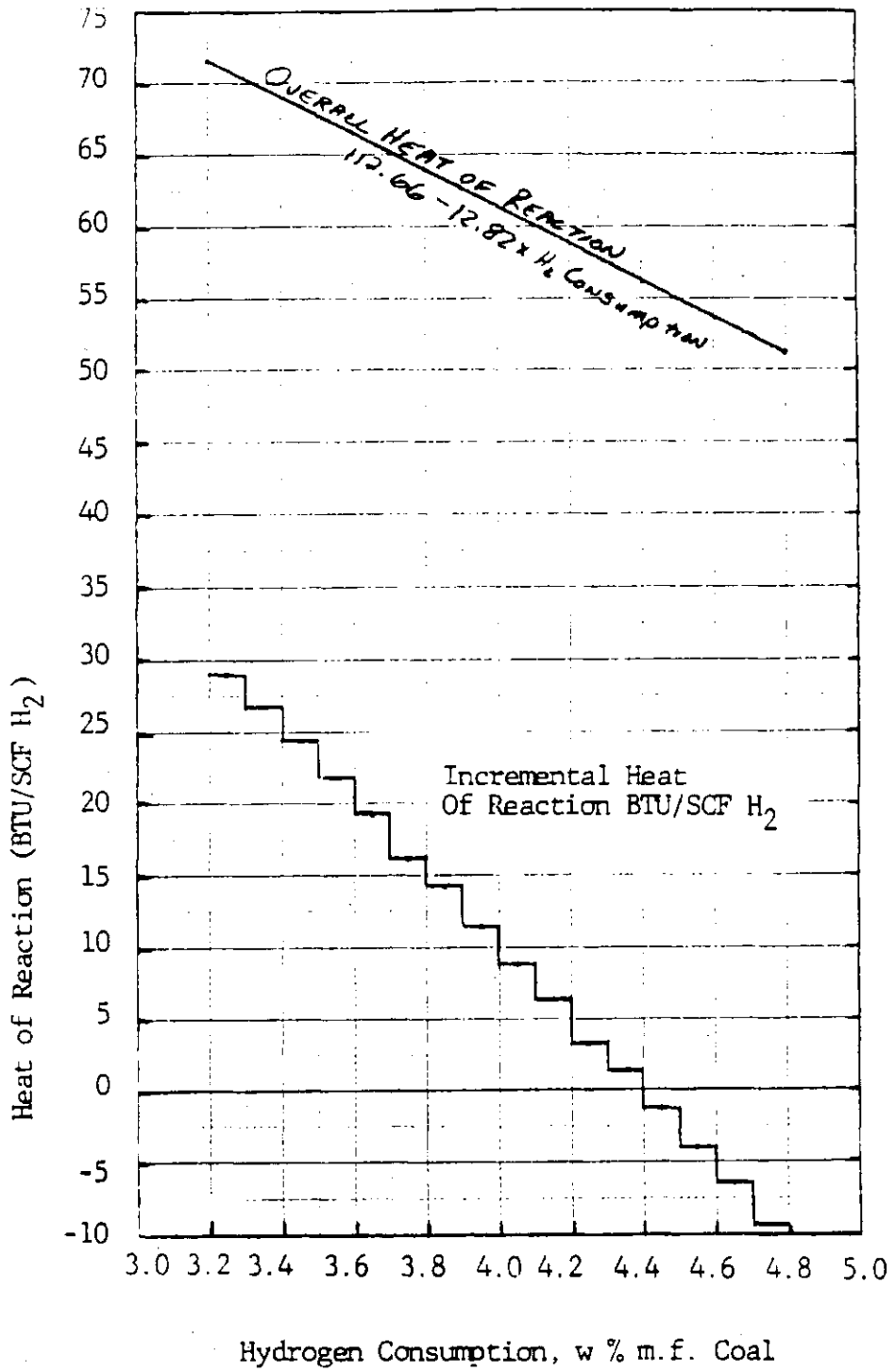

FIGURE 24

COMPARISON OF P-99 DISSOLVER TEMPERATURE PROFILE FOR THE 10 FT AND 20 FT TALL REACTORS

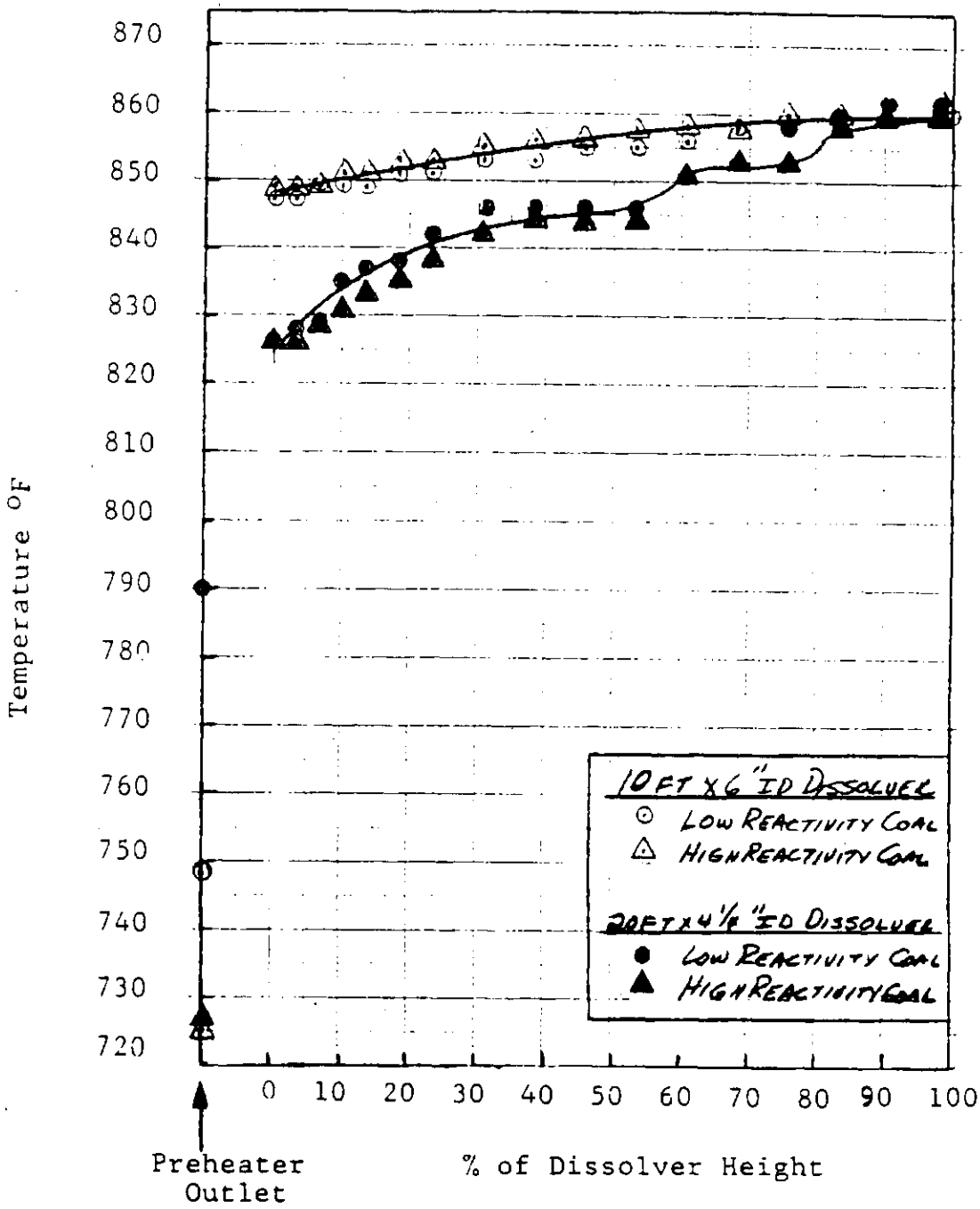

FIGURE 29

Comparison of Observed and Estimated Hydrogen Consumption for A-1 Mass Transfer Tests

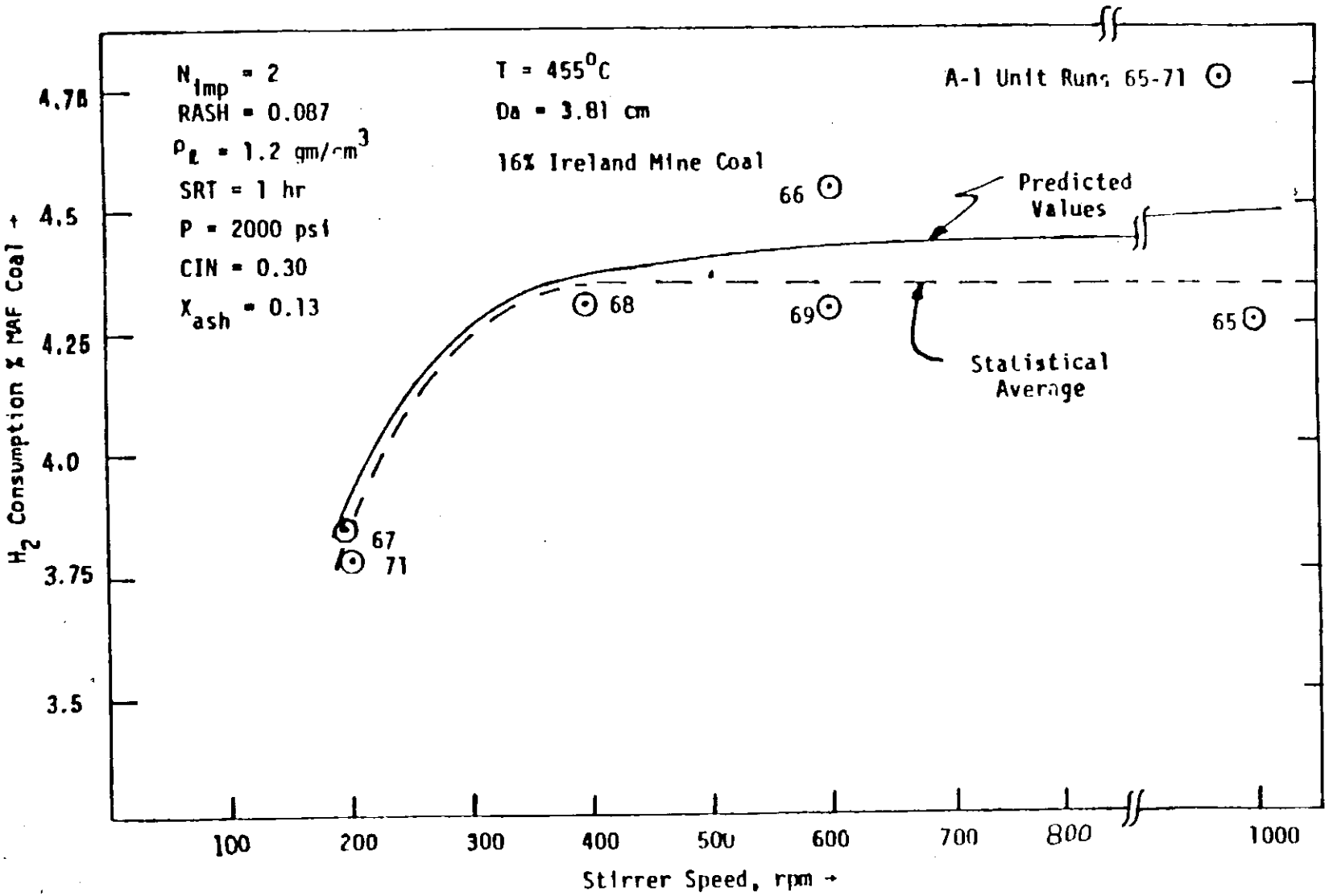

FIGURE 26

FRACTIONAL DECREASE IN HYDROGEN CONSUMPTION (f)
AS A FUNCTION OF SPECIFIC MIXING POWER (P/V)

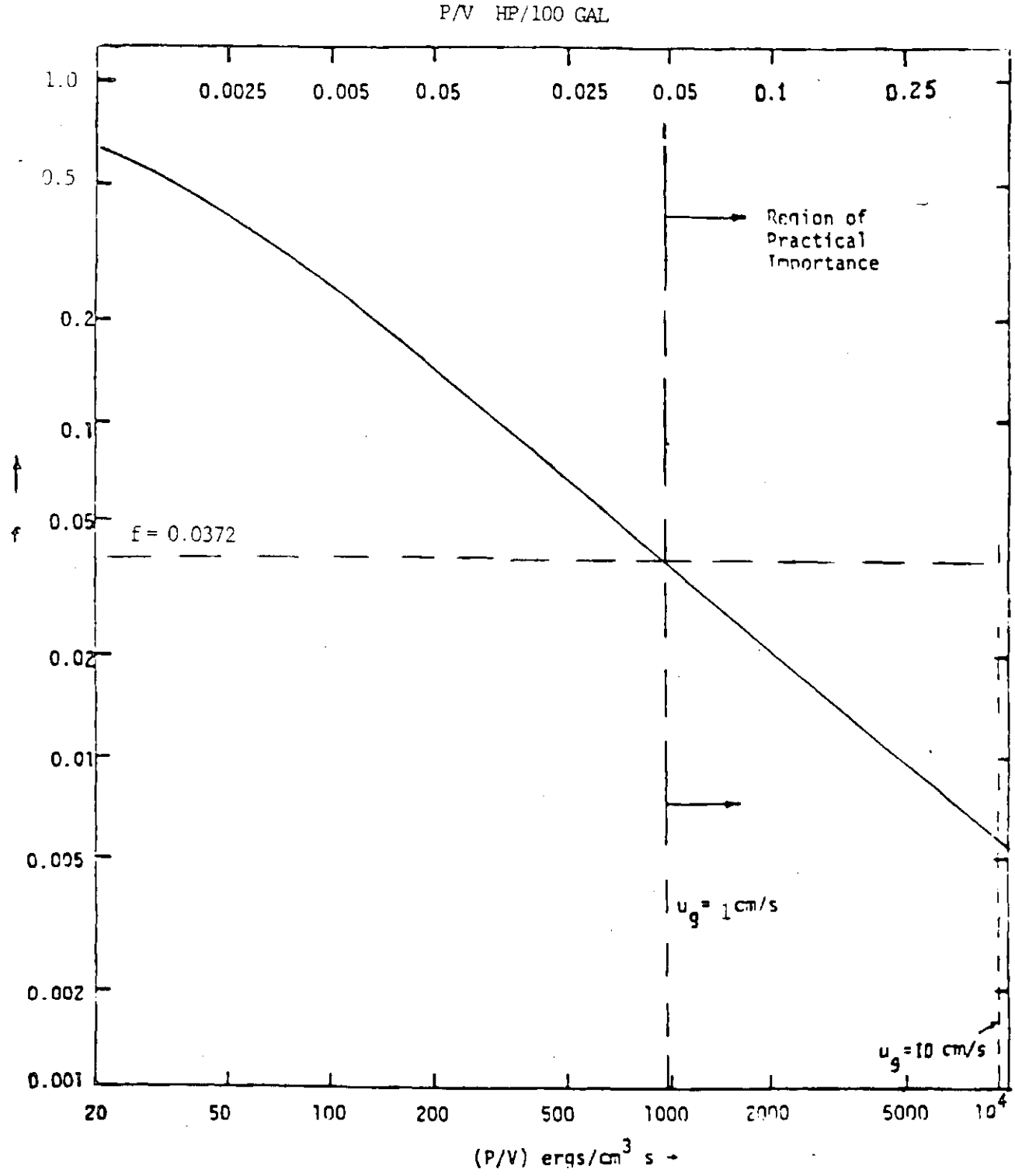

FIGURE 27

EFFECT OF MASS TRANSFER COEFFICIENT ON
FRACTIONAL DECREASE IN HYDROGEN CONSUMPTION (f)

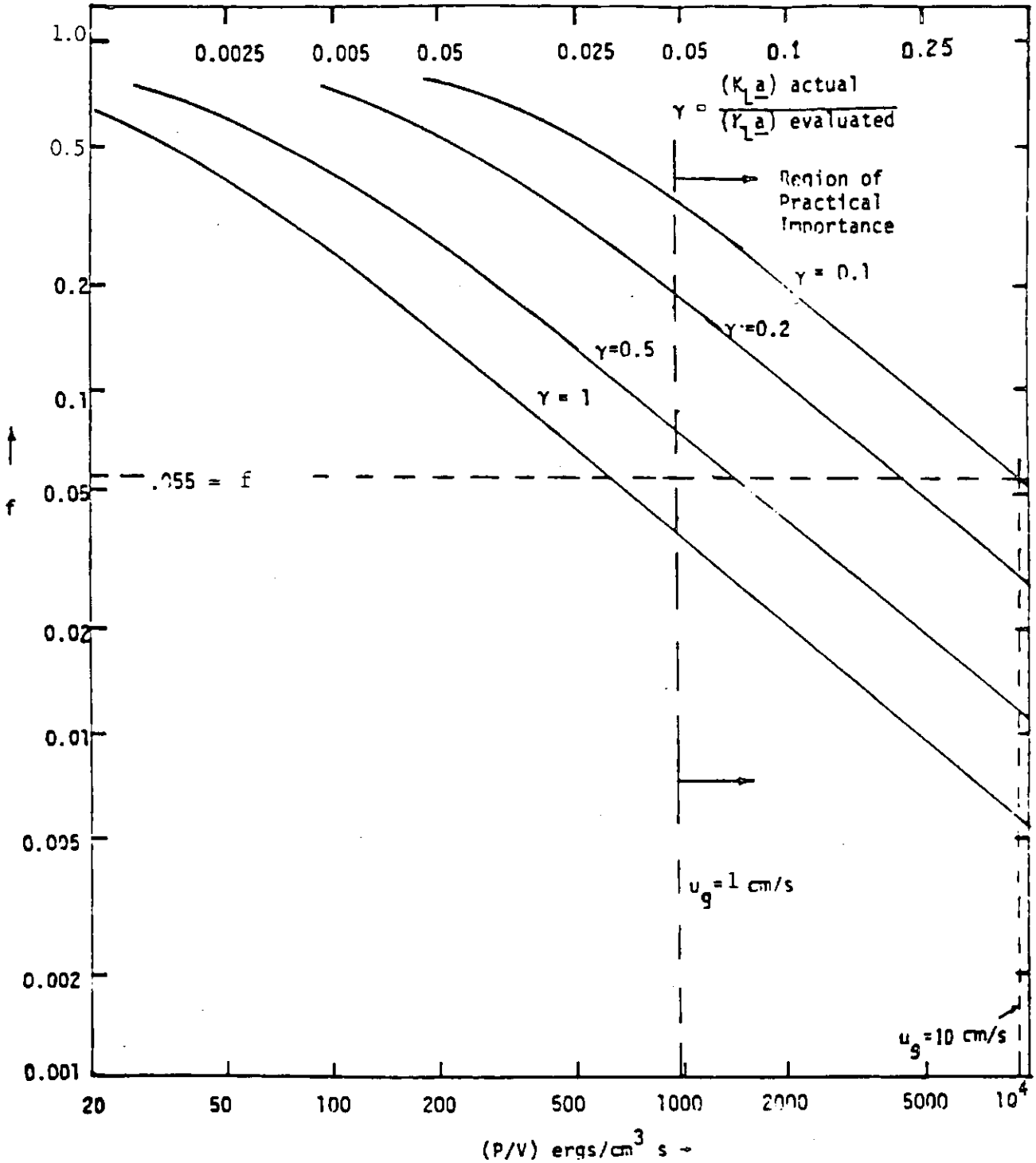

☆ U.S. GOVERNMENT PRINTING OFFICE: 1984-544-063/10325